Green Biocompatible Method for the Synthesis of Collagen/Chitin Composites to Study Their Composition and Assembly Influence on Fibroblasts Growth

A green biocompatible method for the synthesis of collagen/chitin composites to study their composition and assembly influence on fibroblasts growth

Marianna Barbalinardo,[a] Michele Biagetti,[b] Francesco Valle,[a,c] Massimiliano Cavallini,[a] Giuseppe Falini,[b] and Devis Montroni*[b]

[a] National Research Council (CNR), Institute for Nanostructured Materials (ISMN), Via P. Gobetti 101, 40129 Bologna, Italy.

[b] Dipartimento di Chimica "G. Ciamician", Alma Mater Studiorum − Università di Bologna, via F. Selmi 2, 40126 Bologna, Italy.

[c] Consorzio Interuniversitario per lo Sviluppo dei Sistemi a Grande Interfase (CSGI), ISMN-CNR, 40129, Bologna, Italy.

e-mail: devis.montroni@gmail.com

Abstract

A new green biocompatible route for the deposition and/or simultaneous assembly, by pH increment, of collagen/chitin composites is proposed. Both assembled and not-assembled samples with different collagen/chitin ratios were synthesized, maintaining the β-chitin polymorph. The first set showed a micro-fibrous organization with compositional sub-micron homogeneity. The second set presented a nano-homogenous composition based on collagen nano-aggregates and chitin nano-fibrils. The sets were tested as scaffold for fibroblasts growth (NIH-3T3) to study how composition and assembly affect the cell growth. The evidences from the not-assembled scaffolds suggest that the collagen positive influence on cell growth mostly wears out in 48 h, while the addition of chitin appears to enhance this effect for over 72 h. The assembled samples, instead, showed a general higher viability at 24 h but a less positive effect on viability along the time. This was imputed to less available collagen or polysaccharide domains that mediate cell adhesion. The development of this new route for these composites synthesis avoids the use of harmful solvents and allows the simultaneous assembly of these two macromolecules. Moreover, this work highlights critical aspects of the influence that composition and assembly have on fibroblasts growth, a knowledge exploitable in scaffold design and preparation.

Keywords: chitin, collagen, composite, fibroblast, assembly, green chemistry.

Introduction

Collagen is one of the most diffused proteins in the animal kingdom, usually found in connective and mineralized tissues.[1–8] In humans, collagen, especially collagen type I, is mostly associated to cartilages and bones, due to its positive influence on mineral deposition and high mechanical resistance.[1,5,6,8–10] Considering its deep implication in tissues, this protein has been widely applied in material science, exploiting its remarkable biocompatibility, for regenerative medicine.[11–13]

Chitin, on the other hand, is a polysaccharide based on N-acetyl-glucosamine characterized by a high mechanical resistance.[14–18] This biopolymer is the most diffused biopolymer among the existing species and is commonly found in mechanical resistant and supportive structures.[19,20] In mollusks, arthropods, and Porifera is also frequently associated to a mineral phase.[20–22] In these, chitin, mostly in the β-chitin polymorph, has been observed having a strong influence on both biocalcification and biosilification.[9,23,24] Moreover, the biocompatibility of this polymer promoted its use as material for medical application, from drug delivery to wound healing and regenerative medicine.[25–29] The combination of these properties makes chitin a perfect candidate for bone and cartilage regeneration. In fact, labelling studies on rabbits by Ge et al. (2004) showed how a chitinous matrix not only promoted the osteoblasts proliferation, but also recruited the ingrowth of surrounding tissues.[27] Another interesting effect of chitin is the formation of granulation tissue with angiogenesis.[30] It has also been reported that chitin and its metabolites induce fibroblasts to release interleukin-8, which is involved in migration and proliferation of fibroblasts and vascular endothelial cells.[25,31,32]

Compared to other biomacromolecules, chitin is not very good as scaffold for cell growth and proliferation. For this reason, different blends with other materials have been studied.[32–37] Among them, the most important are with collagen.[32,33] In this composite chitin provides an

increased mechanical resistance while collagen enhance the formation of a uniform tissue. In fact, despite good results were obtained using a collagen-based material, Li et al. (2006) reported how the implant on a goat showed a perfect recovery only when reinforced with chitin.[32] The same group reported an increment in the growth rate of mesenchymal stem cells testing a different composite based on chitin and collagen.[37]

Another common feature of these two biomacromolecules is their pH-responsive self-assembly. This process is well known for collagen as it leads to precisely organized fibers.[38,39] Chitin self-assembly, on the other hand, has been studied for the first time in 2019 moving from a stable β-chitin nano-fibril dispersion to uniaxial organized micro-fibers.[40] The simultaneous self-assembly of both these two components in a water-based solvent has never been reported before.

The present work provides two distinct goals. (i) The first one is the development of a new green and fully biocompatible route of synthesis for this composite. This new methodology is carried out entirely in water, without the use of any harmful solvent. This is especially important for chitin, which is commonly manipulated using strong polar organic solvents, usually cytotoxic. This method also allows the assembly of chitin and collagen together by simply rising the pH of the solution. (ii) The second one is to study the influence of collagen/chitin ratio and assembly on fibroblasts. This would help understand how to optimize future collagen/chitin composites to obtain an optimal cell growth. This new method, and the information derived from it, could give a fresh field for the development of greener and more biocompatible materials for medical applications.

Materials and methods

Materials All reagents and solvents were purchased from Sigma Aldrich and utilized without any further purification. A type I collagen from bovine Achilles tendon was used in this study. Squid pens

from *Loligo vulgaris* were collected from a local market. Once hydrated, the lateral blades were isolated, cleaned with distilled water and ethanol 70 vol.%, and then stored dry.

β-Chitin purification from the squid pen The β-chitin was purified from the squid pen of *L. vulgaris* by alkaline deproteination.[14] This was done by inserting 2.5 g of washed squid pens in 100 mL of a boiling 1 M NaOH solution, and stirring for 1 h. After that, the solution was changed with a fresh 1 M NaOH solution and refluxed for another 1 h. The obtained chitin films were washed at room temperature first with a 1 M NaOH solution and then with distilled water until the washing solution had neutral pH. The chitin films were stored dry in a desiccator.

Synthesis of the self-assembled composites For the synthesis of the composites two different dispersions of β-chitin nano-fibrils (β-CnFs) and collagen were initially prepared. The 1 $mg \cdot mL^{-1}$ β-CnFs dispersion was prepared according to what reported in Montroni et al..[40] Briefly, a homogeneous dispersion of β-CnFs was obtained by placing 100 mg of β-chitin, cut into about 0.5 cm^2 square pieces, in 100 mL of an acetic acid solution at pH 3. The solution was stirred vigorously for 72 h at room temperature.

The 1 $mg \cdot mL^{-1}$ collagen dispersion was prepared by adding 200 mg of collagen in 40 mL of a pH 3 acetic acid solution. The dispersion was stirred overnight and then centrifuged at 2000 g for 5 min. After centrifugation, the supernatant was collected, and the pellet was dispersed in 20 mL of solvent and stirred again for 2 h. The dispersion was centrifuged again collecting the supernatant with the previous one. The process was repeated once or twice, depending on the amount of insolubilized collagen. The remaining pellet (usually between 5 and 20 mg) was dried, weighted, and disposed. The dispersion collected along the different steps was properly diluted, basing on the weight of the collagen lost in the pellet, to get a 1 $mg \cdot mL^{-1}$ final concentration of collagen.

The collagen/chitin mixtures were prepared by mixing 1 $mg \cdot mL^{-1}$ chitin and 1 $mg \cdot mL^{-1}$ collagen, both in acetic acid pH 3, in different ratios. In the assembled samples the self-assembly was induced by changing the pH of 20 mL of the mixture. The pH change was induced using NaOH 10 M, and NaOH 1 M for fine adjustments. pH was measured using a pH-meter BASIC 20 (pH ± 0.01) by Crison Instruments coupled with a HI1048 pH electrode (Hanna Instruments). The pHmeter was calibrated daily. Both the assembled (added with NaOH) and not assembled solutions were left for 24 h at room temperature (25 °C) without any stirring. The samples were then frozen with liquid nitrogen and lyophilized using a FreeZone® 1 (Labconco Corp., Kansas City, MO, US). The obtained material was compacted to obtain a film, washed with distilled water, and dried between two glass slides in a desiccator. Due to the high amount of sodium acetate formed the assembled samples frequently needed one or two extra washing steps. These washing steps were not performed on the not assembled samples to avoid as much as possible to induce assembly.

Microscopy analysis on the composites Optical microscopy images were collected using a SM-LUX POL microscope equipped with a 5.0 MP Moticam 5 camera. The samples were observed right after the end of the 24 h, before the freeze-drying. The sample was stirred, a drop of sample was collected and placed on a glass microscope slide, covered with a glass cover slip, and observed immediately. AFM was carried on at the SPM@ISMN facility using a Multimode VIII microscope equipped with a Nanoscope V controller (Bruker, Santa Barbara, CA, US). Briefly, the dispersions where deposited onto freshly cleaved mica and let dry. In some cases, the sample was additionally rinsed with an acetic acid solution at pH 3 and dried with a gentle stream of clean nitrogen. Images were collected in ScanAsyst mode using SNL-10 tips (nominal spring constant 0.35 $N \cdot m^{-1}$ and nominal resonance frequency 65 KHz). The analysis was performed using Gwyddion, an open access software to perform the basic manipulation (plane fit and zero level setting).[41]

SEM images were acquired with a Philips SEM 515 using a tension of 15 kV. The dry samples were glued on carbon tape, dried overnight in a desiccator, and coated with 20 nm of gold prior to image them.

Structural analysis The attenuated total reflectance Fourier-transform infrared spectroscopy (ATR-FTIR) spectra were collected using a Nicolet IS10 spectrophotometer. Omnic software (Thermo Electron Corp., Woburn, MA) was used for data processing. The dry samples were analyzed by ATR with 2 cm^{-1} resolution and 70 scans using a germanium crystal.

X-ray diffraction (XRD) patterns were collected using a PanAnalytical X'Pert Pro diffractometer equipped with multi array X'Celerator detector using Cu Kα radiation generated at 40 kV and 40 mA (λ = 1.54056 Å). The diffraction patterns were collected in the 2θ range between 4 ° and 25 ° with a step size (Δ2θ) of 0.05 ° and a counting time of 100 s. Each pattern collection was repeated at least twice on different samples.

Cell cultures Mouse embryonic fibroblast (NIH-3T3) cells were cultured under standard conditions in the DMEM medium, supplemented with 10 vol.% FBS, 2 mM L-glutamine, 0.1 mM MEM Non-Essential Amino Acids (NEAA), 100 $U \cdot mL^{-1}$ penicillin, and 100 $U \cdot mL^{-1}$ streptomycin in a humidified incubator set at 37 °C with 5 % CO_2. Cells were seeded on samples at a density of 10^5 $cells \cdot cm^2$.

Cells viability test using a resazurin reduction assay Cell viability was determined by resazurin reduction assay; the reagent is an oxidized form of the redox indicator that is blue in color and non-fluorescent. When incubated with viable cells, the reagent is reduced and it changes its color from blue to red becoming fluorescent. Briefly, cells were seeded on samples with complete medium. After incubation times, the resazurin reagent was added directly to the culture medium with 10

vol.% of medium contained in each sample and incubated for 4 h at 37 °C with 5 % CO_2. Subsequently, aliquots from each sample were transferred to a 96 multiwell plate for fluorescence measurement at λ_{exc} 560 nm and λ_{em} 590 nm (Thermo Scientific Varioskan Flash Multimode Reader). A negative control of only medium without cells was included to determine the background signal along with a positive control of 100 % reduced resazurin reagent without cells.

Fluorescence microscopy (Actin and nucleus staining) on fibroblasts Cells were fixed with 4 vol.% paraformaldehyde in DPBS, washed with DPBS. They were then permeabilized with 0.001 wt.% Triton-X 100. The cells were labelled with TRITC-conjugated phalloidin (FAK100, Merck Millipore) for 1 h, followed by rinses with DPBS. Actin staining was critical to map local orientation of actin filaments within cells. Nuclear counterstaining was performed by incubation with DAPI (FAK100, Merck Millipore) for 3 min, followed by rinses with DPBS. Samples were examined using a Nikon Eclipse 80i microscope equipped for fluorescence analysis.

Statistical Analysis All data represented the mean ± standard deviation (SD). Statistical significance was determined using a one-way analysis of variance with Turkey's test for multiple comparisons using Origin 8 software (OriginLab corporation). Differences were considered significant when $p < 0.05$, $p < 0.005$m, and $p < 0.001$.

Results

Self-assembly and material characterization

The assembly of chitin nanofibrils in water, as discussed in Montroni et al. (2019), is different depending on the pH environment where it takes place.[40] At pH 3 no assembly was observed,

leading to a disorganized mass of fibrils. At pH 8 the best condition for chitin assembly occurs, leading to about 10 μm thick fibers.

In this study, a 1 mg·mL^{-1} chitin nano-fibril dispersion was mixed with a type I collagen dispersion of the same concentration to obtain mixtures with different mass ratios. The 1 mg·mL^{-1} concentration was chosen for its tendency to give longer fibers and for practical reasons.[40] The different collagen/chitin mass ratios investigated are reported in Table 1.

Table 1: Composition of the composite materials prepared and investigated. The total amount of material was constant.

Sample	**Chitin / wt.%**	**Collagen / wt.%**
C100	100	0
C75	75	25
C50	50	50
C25	25	75
C00	0	100

The result of the assembly process was studied 24 h after increasing the pH of the dispersion to 8, being both chitin and collagen pH responsive. As can be observed in Figure 1, neither chitin nor collagen formed micro-fibers at pH 3. Contrary, at pH 8 both chitin and collagen assembled. Chitin assembled in long highly birefringent fibers with a preferential axial organization. On the other hand, collagen formed less birefringent fibers highly aggregated and with a lower axial organization. Intermediate samples showed a gradual interconversion between the two kinds of assembly and associated morphologies. Observing the fibers using a constant exposure and gain of the optical microscope system setup, the increase of fiber birefringence along the samples was coherent with

the increment in chitin content, moving from more birefringent chitin fibers to less birefringent collagen ones.

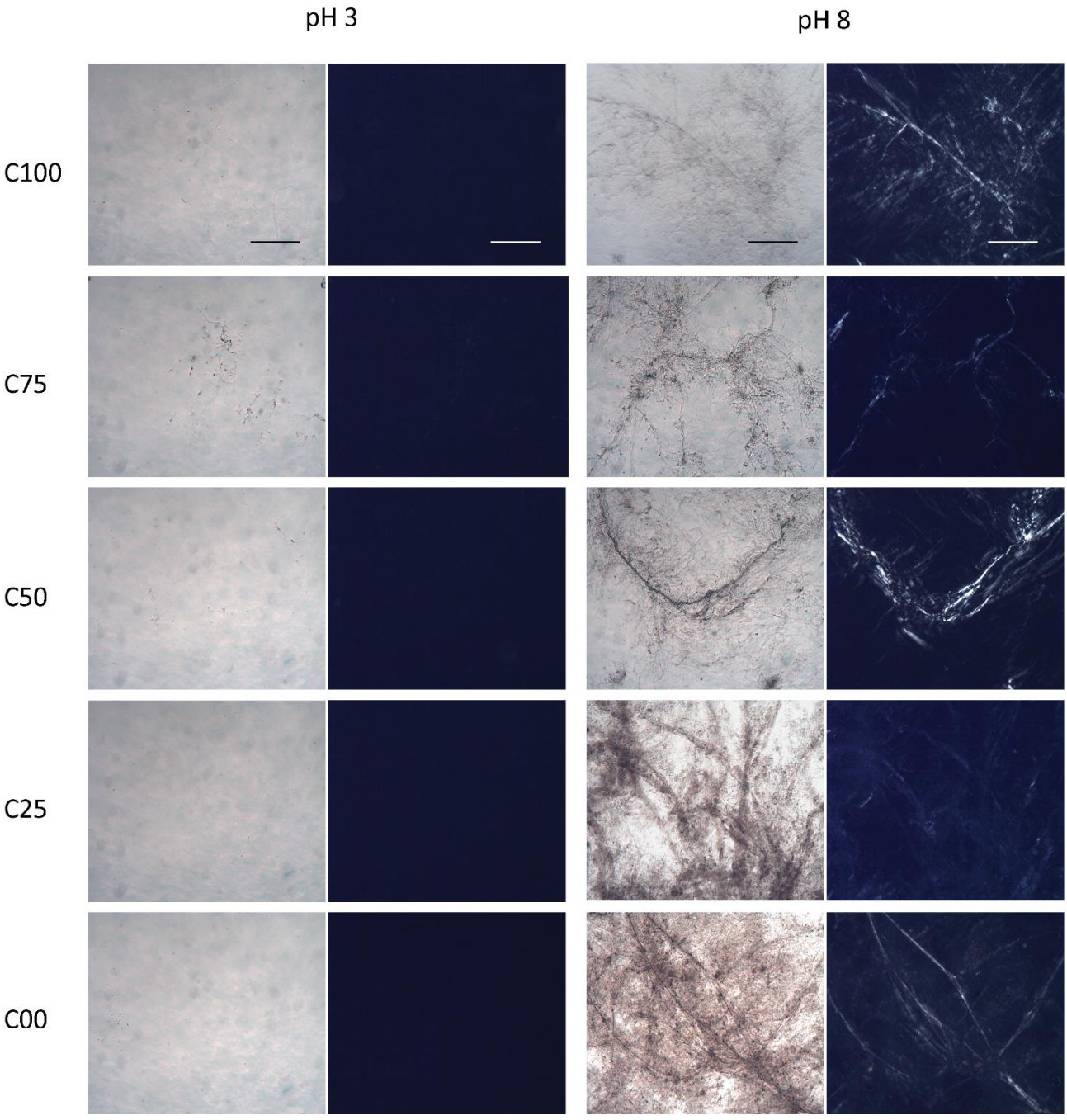

Figure 1: Optical microscopy images of the collagen/chitin mixtures in water at the two pHs studied, 3 and 8. For each condition, an optical image and one with cross-polarizers are reported. Scale bar 300 µm.

The different mixtures in water solution at pH 3 were also analyzed using AFM, Figure S3. Nanofibrils, as the one observed in Montroni et al. (2019), were observed increasing the chitin amount in the samples, being the only component in C100.[40] These fibrils were not observed in C00. Instead, the presence of collagen aggregates was observed.

The dry samples were examined using FTIR and XRD to evaluate the interaction between the two biopolymers composing the materials. The ATR-FTIR spectra (Figure S1) of C00 and C100 showed the typical absorption bands of chitin and collagen, as reported in the literature. The major absorption bands associate with collagen were amide I (1653 cm^{-1}), II (1544 cm^{-1}), III (1237 cm^{-1}), A (3321 cm^{-1}), and B (3080 cm^{-1}).[42] Chitin showed intense absorption bands for amide I (1653 cm^{-1}) and II (1558 cm^{-1}), CH bending (1374 cm^{-1}), four signals related to ring stretching (1155 cm^{-1}, 1112 cm^{-1}, 1069 cm^{-1}, and 1031 cm^{-1}), N-H stretching (3277 cm^{-1}), and O-H stretching (3447 cm^{-1}).[14] Moving from C100 to C00 an increase in the relative intensity of the collagen absorption bands was observed along with a decrease of the chitin ones. The collagen and chitin absorption bands showed no shifts. Comparing the two pH conditions, the composites prepared at pH 3 showed changes in the relative intensity of some absorption bands, compared to the amide I absorption band, increasing the chitin content of the sample. An increase of the absorption bands related to O-H stretching, N-H stretching, amide II (generally associated to a combination of N–H bending and C–N stretching vibrations), and CH_2 bending (1413 cm^{-1}), and a decrease of CH_3 (2924 cm^{-1}) and CH_2 stretching (2853 cm^{-1}) were observed. The XRD (Figure S2) diffractograms of pure chitin (C100) showed peaks at 8.4 ° and 19.5 ° of 2Θ at pH 3 and 8. Pure collagen (C00) presented a diffraction peak at 7.6 °, associated with the intermolecular lateral packing distance between collagen molecular chains, and a broad peak around 20 °, attributed to the diffuse scattering.[42,43] At both the pHs the 8.4 ° chitin diffraction peak and the 7.6 ° collagen diffraction peak appeared to coexist in the composites, being one overlapped to the other. The 19.5 ° chitin diffraction peak, instead, got

broader increasing the collagen amount until it completely interconverted in the broad collagen diffraction peak.

Once filmed, the dry material was analyzed using SEM to study the sample morphology that directly interfaces with the cells. The images, reported in Figure 2, show an almost uniform smooth surface for the samples at pH 3 with a fibrillar appearance at the sub-micron level. Moving to chitin-rich samples a layered textural organization arises. The samples at pH 8, instead, showed a fibrous organization. Only C00 showed the typical pattern of collagen assembly, while only few little fibers were visible at pH 3.[1,8] Also in this condition, increasing the chitin content, a layer organization was observed along with the formation of ribbon-like structures of increasing width.

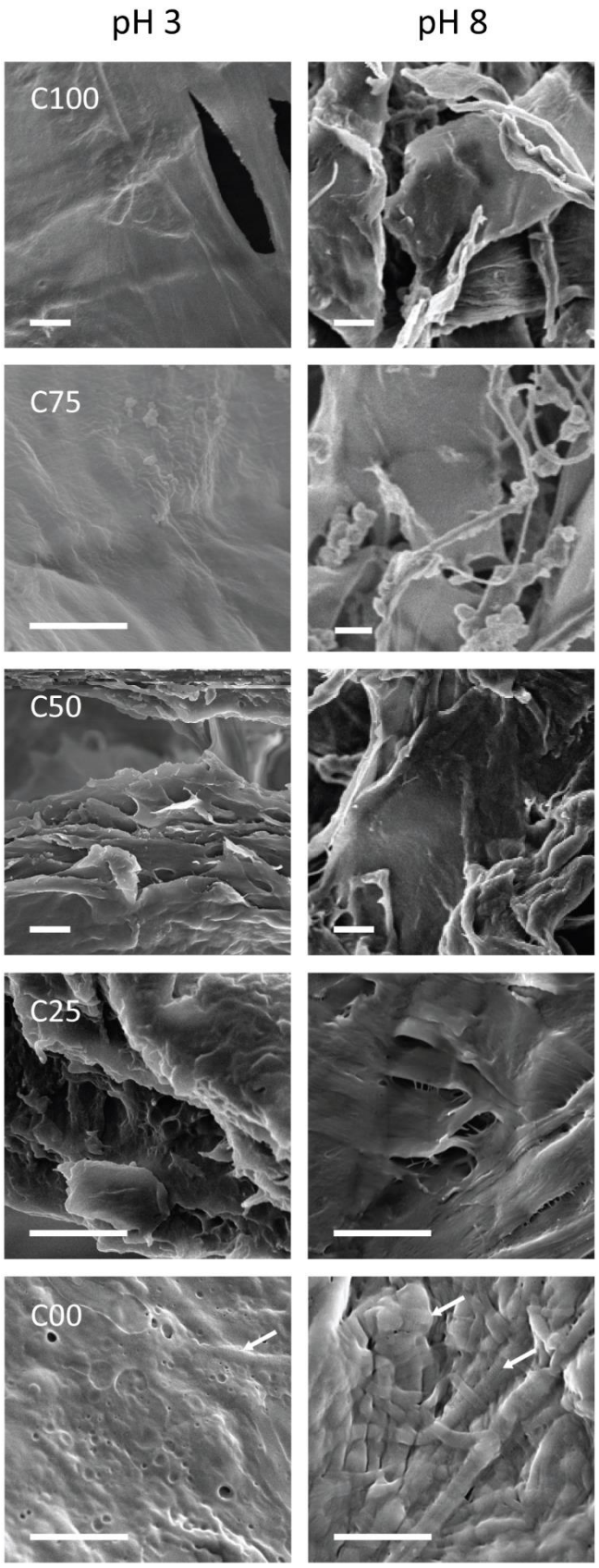

Figure 2: SEM images of the different composites. In C00 white arrows indicates the typical collagen assembly pattern. Scale bar: 2 µm.

Evaluation of cell viability and proliferation

NIH-3T3 cells were used to evaluate the cell response to the presence of the collagen/chitin composite. The cell viability on the different composite materials was tested using fibroblast at 24 h, 48 h, and 72 h, as reported in Figure 3. The results were normalized on the viability at 24 h for the C00 sample. Compared to a control sample without any matrix, the cell viability was slightly higher using collagen assembled at pH 8 rather than the one at pH 3 (105 ± 4 % and 98 ± 6 % respectively). The results using the matrices prepared at pH 3 showed an increment in viability increasing the collagen amount at 24 h, being C100 the one with the lowest viability (42 ± 7 %). At 48 h an increment in viability of about 25-30 % was observed in all the samples except C25. Passing from 48 h to 72 h the highest increments, of 10-15 %, in viability were observed for C25, C75, and C100; the pure collagen sample, C00, increased by 4 ± 4 % being probably close to a plateau. As absolute value, the samples C25, C50, and C75 showed a similar viability at 72 h, between 110 % and 120 %, while the pure collagen matrix was about 130 %. The samples assembled at pH 8 showed a different trend. At 24 h all the samples except the pure collagen showed a comparable viability, between 74 % and 85 %. At 48 h an increment of 20-25 % in viability was observed in C00, C25, and C50; C100 showed instead a decrement of 6 ± 3 %. Between 48 h to 72 h, no increment in viability was observed with only C25 being almost stable at the 48 h value.

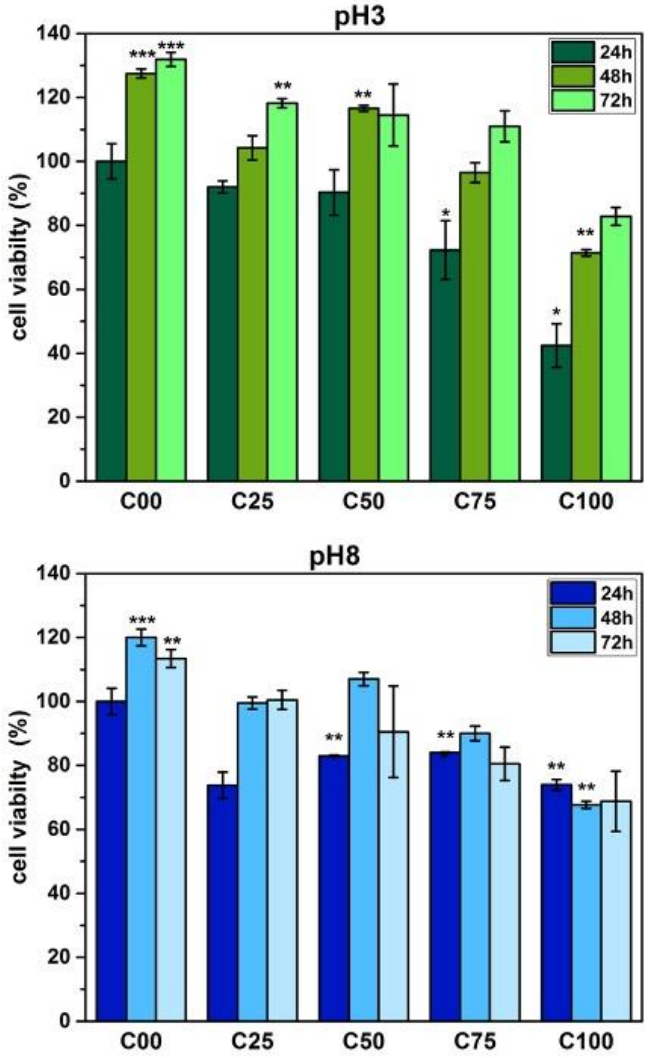

Figure 3: Cell viability at 24 h, 48 h, and 72 h in the presence of the samples prepared at pH 3 and 8. For each sample set the results are normalized on the viability at 24 h for the C00 sample. Data represent the mean ± SD. Statistical analyses were performed using ANOVA followed by Turkey's test. *p < 0.05, **p<0.005 and ***p < 0.001 denote significant differences respect to C00.

Cell adhesion and proliferation are studied at 72 hours on both samples manufactured at pH 3 and pH 8.

In figure 4, after 72 h of incubation a homogenous coverage of cells with a good morphology was observed on C00, C25, and C50 at pH3. Spherical and poorly adhered cells were observed in C100. Cells grown in C75 presented a good morphology, but the scaffold coverage was not homogenous, having few areas with no cells. The right column in Figure 4 shows the observations of cell adhesion

and proliferation on samples at pH 8 after 72 h. C00, C25, C50, and C75 showed cells with a good morphology but poor cell adhesion with incomplete coverage of the sample. The geometry of the sample did not allowed the observation of a wide area of sample as on samples prepared at pH 3. Sample C100 showed the same cell organization as at pH 3 at 72 h.

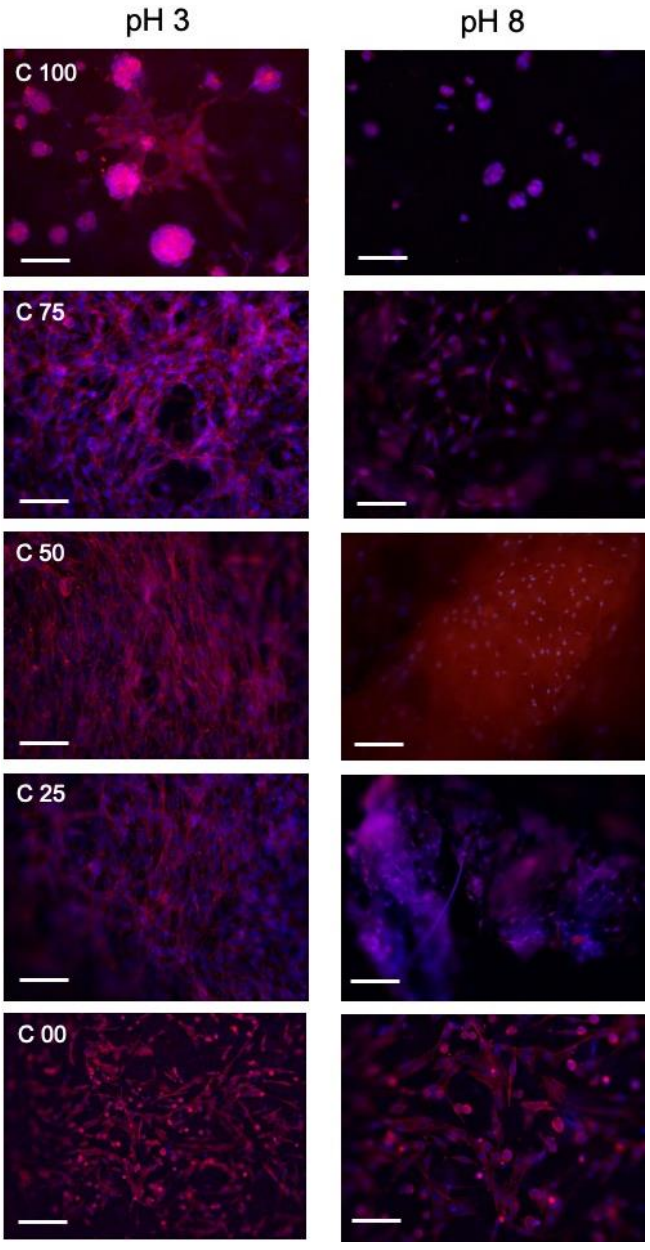

Figure 4: Fluorescence micrographs of NIH-3T3 on different composites. Cells were labeled specifically for actin (red) and the nucleus (blue) after 72 h of incubation. Scale bar 100 µm.

Discussion

Study of the material synthesis

In this study we focused on two goals. The first was to investigate a new method to synthesize collagen/chitin composites without using harmful solvents. Since this new method implies chemical conditions that allow inducing the assembly of both these biomacromolecules, a study on their simultaneous assembly was performed too.

Two pH values were studied after 24 h from the mixing of the two biopolymers: pH 3 as a condition where no assembly takes place; pH 8 as an optimal condition for the assembly. The resting time of 24 h was selected as a time long enough to allow the complete equilibration of the assembly process.[40] By observing the optical microscopy images, micro-fibers were visible only at pH 8. Since optic microscopy was not appropriate in resolution to investigate the material obtained at pH 3, AFM was used to evaluate eventual micro- and nano-scale assembly. Nanofibrils were observed and associated to chitin, while nano-aggregates were associated to collagen. In literature, some studies report that the critical concentration in solution above which collagen molecules aggregate is 0.5 $mg \cdot mL^{-1}$.[42,44] The working concentration was 1 $mg \cdot mL^{-1}$, so we could assume those nano-aggregates were collagen-based. Despite the presence of collagen aggregation, optical microscopy and AFM techniques showed at pH 3 a homogenous dispersion of the two biomacromolecules.

At pH 8, the optical microscopy images showed that the fibers shifted from a chitin- to collagen-like morphology increasing the relative amount of the components, without any evidence of separate domains of assembly. The same effect was observed on the fiber birefringence.

Considering the position of the diffraction peaks and the shape of the amide I absorption band (split in α-chitin) in C100, chitin maintained the β-chitin polymorph in all the experimental conditions.[14,40,45,46] This is an important milestone in collagen/chitin composites, since not

many works treat this polymorph even if is involved in many biological processes, among which biomineralization is the best known.[33]

Comparing pH 3 and pH 8 FTIR spectra, the differences in relative intensity observed in the FTIR chitin absorption bands were mostly associated to amine related signals (C-N or N-H vibrations) and hydrophobic groups (C-H vibrations). This might be due to an incomplete deprotonation of the amine groups (the degree of acetylation of chitin was about 89 %)[14] at pH 3 and a consequent change in the hydrophobic regions.

Contrary to what observed using optic microscopy and AFM, XRD showed a peak at 7.6 ° associated with the intermolecular lateral packing distance between collagen molecular chains.[42] Using SEM, submicron assembled regions were observed in C00 at pH 3. These regions might be responsible for the peak observed in XRD. Since they are limited in number and dimension, these submicron structures were not visible using AFM and optical microscopy. Considering that no assembly occurred during the 24 h at pH 3, we can assume that these assembled regions are derived from suspended collagen fibers. Despite that, the microscopy techniques applied suggest the matrices obtained at pH 3 are almost nano-homogenous materials.

The absence of peak shifts in the FTIR spectra and XRD analysis in both pHs suggests chitin and collagen do not interact in ways that can alter their molecular structure or crystalline packing. Despite the absence of evidences for co-assembly, the formation of uniform fibers observed in the optical images of the composites implies some interactions between the two biopolymers. Observing the SEM images, collagenous fibers were observed only in C00 at pH 8. The other composites, instead, showed a morphology more similar to C100. In 2019, Moon et al. studied the interaction between collagen and chitin, derived from β-chitin, in an electrospun composite.[47] In their work, the 2DCOS analysis on FTIR spectra showed favorable intra-molecular hydrogen bonds between the two biopolymers. In our work, the assembly was carried out without any stirring, for

this reason we assumed mechanical entanglement was not driving this sample homogeneity. The combination of these observations implies that the interaction between the two biopolymers leads to a submicron homogenous material after the assembly.

Fibroblasts growth on the scaffolds

The second goal of this study was to investigate how the composition and assembly of collagen/chitin composites influence fibroblasts growth. For this reason the previously investigated not-assembled (pH 3) and assembled (pH 8) matrices with variable composition were tested as scaffold for cell growth.

Fibroblasts viability on scaffolds prepared at pH 3 showed an overall positive trend during the 72 h examined. A higher increment in viability was observed increasing the chitin amount. At the end of the 72 h, pure collagen seemed to be closer in reaching a plateau in viability compared to chitinous composites. This plateau was associated with the appearance of spherical morphologies in the cells, an index of a lower adhesion to the substrate. On the other hand, cells with a good morphology were observed appearing at 72 h on pure chitin. This evidence suggests that chitin's positive influence on cell growth, which is enhanced when associated to collagen, is slowly increasing and becoming more persistent along time. On the contrary, collagen shows a fast positive influence on cell growth that quickly reaches a plateau.

Cells grown on the matrices prepared at pH 8 showed a more positive influence on cell viability within 24 h, higher than that observed using the samples prepared at pH 3. At 72 h a proper cell morphology, but poor coverage of the scaffold, was observed. Despite that, between 48 h and 72 h cell viability seems to invert its trend, which became negative. The only exception was observed on pure chitin, where cells appear to not develop properly and the viability has an unchanged negative trend.

Despite assembled samples showed a higher viability within 24 h, the positive trend observed on not-assembled samples allows these last to overpass their assembled counterpart in 72 h. (i) This difference might arise from the higher compositional homogeneity of the pH 3 samples. (ii) Another possible explanation might come from sodium acetate residues adsorbed into the assembled matrices. This last possibility is anyway unlikely to be, since all samples were incubated at 37 °C with 5 % of CO_2 in the growing medium, which did not show any evidence of pH-related color variation, for 24 h before using them in cell-related experiments. (iii) Increasing chitin led to an almost unchanged cell viability incremental trend in not-assembled composites, while an almost linear decrement was observed in assembled samples increasing chitin content. This might suggest another possible explanation. During the assembly process, chitin might have covered collagen assembled domains, making them less available. (iv) Comparing the pure chitin samples, a positive influence was observed on the not-assembled sample, while the assembled one showed a slight negative trend. This difference might arise from the diverse bioavailability of chitin nanofibrils in the not-assembled sample. Their availability might induce a higher viability of cells due to carbohydrate-protein interaction (e.g. selectins) that mediate the adhesion.[48,49] The absence of this effect might be the reason why pH 8 prepared samples did not appear to benefit of the long-term positive effect of chitin as samples prepared at pH 3. This last explanation is supported by the fact that C25 was the only sample that never reached a negative trend in viability, probably because chitin fibrils were less assembled and more homogenously dispersed in the collagen matrix making them more available.

Conclusion

In the first section of this research, a new method for the green synthesis of collagen/chitin composites without using cytotoxic solvents was proposed. This method also enables the

simultaneous assembly of both biomacromolecules increasing the pH of the dispersion, while conserving the β-chitin polymorph. The not-assembled samples appeared to have a nano-homogenous composition based on collagen nano-aggregates and chitin nano-fibrils. The assembled samples, instead, showed a micro-fibrous appearance combined with a submicron homogeneity in the composition. No evidence at the structural level of co-assembly were observed. Experimental evidences from the not-assembled scaffolds suggest collagen positive influence on cell growth mostly wear out in the first 48 h. On the other hand, the addition of chitin appears to enhance this effect for over 72 h. The combination of these two influences was mostly emphasized in the specimen with 75 wt.% chitin. This sample showed a viability at 72 h of about 115 % compared to 130 % of pure collagen, but also an overall increment (between 24 h and 72 h) of 40 % (15 % of which between 48 h and 72 h) compared to 30 % of pure collagen (5 % of which between 48 h and 72 h). On the other hand, the assembled samples showed a general higher viability at 24 h but a less positive effect on viability along the time. This might be imputed to less available collagen or polysaccharide domains that might mediate cell adhesion. For this reason, the composite that gave better results has 25 wt.% chitin. This sample showed about 100 % viability at 72 h, about 113 % for pure collagen, and an overall increment in viability of 27 %, about 13 % for pure collagen.

This green and biocompatible method to obtain collagen/chitin composites opens to new routes of synthesis for biomaterials. In future, it could be combined with multiple techniques to cast or shape cell scaffolds, especially for mineralized tissues regeneration thanks to the presence of β-chitin. Moreover, the study on fibroblasts clarifies the combined influence these biomacromolecules have and how assembly, despite being a feasible way to enhance the scaffold mechanical properties, might interfere with it. This knowledge could be easily exploited in future studies on collagen/chitin composites, enabling future research to enhance the performances of their scaffolds.

Acknowledgements

The authors thanks the SPM@ISMN facility for the support in the AFM characterization and Dr. Franco Corticelli (CNR-IMM) for helping acquiring the SEM images. M.B. was supported by the project MIUR-PRIN prot. 2017YH9MRK. F.V. was partly supported by the Horizon 2020 Framework Programme under the grant FETOPEN-801367 evFOUNDRY and under the grant FET Proactive-952183 BOW.

Funding

This research did not receive any specific grant from funding agencies in the public, commercial, or not-for-profit sectors.

Supplementary material

FTIR, XRD, and AFM data reported in the text can be found in the supplementary information.

References

[1] F. Nudelman, K. Pieterse, A. George, P.H.H. Bomans, H. Friedrich, L.J. Brylka, P.A.J. Hilbers, G. De With, N.A.J.M. Sommerdijk, The role of collagen in bone apatite formation in the presence of hydroxyapatite nucleation inhibitors, Nat. Mater. 9 (2010) 1004–1009. https://doi.org/10.1038/nmat2875.

[2] M.T. Dimuzio, A. Veis, The biosynthesis of phosphophoryns and dentin collagen in the continuously erupting rat incisor, J. Biol. Chem. 253 (1978) 6845–6852.

[3] P. Alam, S. Amini, M. Tadayon, A. Miserez, A. Chinsamy, Properties and architecture of the sperm whale skull amphitheatre, Zoology. 119 (2016) 42–51. https://doi.org/10.1016/j.zool.2015.12.001.

[4] R. Seidel, A.K. Jayasankar, M.N. Dean, The multiscale architecture of tessellated cartilage and its relation to function, J. Fish Biol. (2020) 1–14. https://doi.org/10.1111/jfb.14444.

[5] M.P.E. Wenger, L. Bozec, M.A. Horton, P. Mesquidaz, Mechanical properties of collagen fibrils, Biophys. J. 93 (2007) 1255–1263. https://doi.org/10.1529/biophysj.106.103192.

[6] E. Gentleman, A.N. Lay, D.A. Dickerson, E.A. Nauman, G.A. Livesay, K.C. Dee, Mechanical characterization of collagen fibers and scaffolds for tissue engineering, Biomaterials. 24 (2003) 3805–3813. https://doi.org/10.1016/S0142-9612(03)00206-0.

[7] D. Montroni, C. Piccinetti, S. Fermani, M. Calvaresi, M.J. Harrington, G. Falini, Exploitation of mussel byssus mariculture waste as a water remediation material, RSC Adv. 7 (2017) 36605–36611. https://doi.org/10.1039/c7ra06664c.

[8] F. Nudelman, A.J. Lausch, N.A.J.M. Sommerdijk, E.D. Sone, In vitro models of collagen biomineralization, J. Struct. Biol. 183 (2013) 258–269. https://doi.org/10.1016/j.jsb.2013.04.003.

[9] H. Ehrlich, Chitin and collagen as universal and alternative templates in biomineralization,

2010. https://doi.org/10.1080/00206811003679521.

[10] X. Wang, R.A. Bank, J.M. TeKoppele, C. Mauli Agrawal, The role of collagen in determining bone mechanical properties, J. Orthop. Res. 19 (2001) 1021–1026. https://doi.org/10.1016/S0736-0266(01)00047-X.

[11] S.A. Sell, M.J. McClure, K. Garg, P.S. Wolfe, G.L. Bowlin, Electrospinning of collagen/biopolymers for regenerative medicine and cardiovascular tissue engineering, Adv. Drug Deliv. Rev. 61 (2009) 1007–1019. https://doi.org/10.1016/j.addr.2009.07.012.

[12] K. Lin, D. Zhang, M.H. Macedo, W. Cui, B. Sarmento, G. Shen, Advanced Collagen-Based Biomaterials for Regenerative Biomedicine, Adv. Funct. Mater. 29 (2019) 1804943. https://doi.org/10.1002/adfm.201804943.

[13] D. Montroni, F. Valle, S. Rapino, S. Fermani, M. Calvaresi, M.J. Harrington, G. Falini, Functional Biocompatible Matrices from Mussel Byssus Waste, ACS Biomater. Sci. Eng. 4 (2018) 57–65. https://doi.org/10.1021/acsbiomaterials.7b00743.

[14] D. Montroni, S. Fermani, K. Morellato, G. Torri, A. Naggi, L. Cristofolini, G. Falini, β-Chitin samples with similar microfibril arrangement change mechanical properties varying the degree of acetylation, Carbohydr. Polym. 207 (2019) 26–33. https://doi.org/10.1016/j.carbpol.2018.11.069.

[15] H.R. Hepburn, I. Joffe, N. Green, K.J. Nelson, Mechanical properties of a crab shell, Comp. Biochem. Physiol. 50A (1975) 551–554. https://doi.org/10.1016/0300-9629(75)90313-8.

[16] Y. Ogawa, R. Hori, U.J. Kim, M. Wada, Elastic modulus in the crystalline region and the thermal expansion coefficients of α-chitin determined using synchrotron radiated X-ray diffraction, Carbohydr. Polym. 83 (2011) 1213–1217. https://doi.org/10.1016/j.carbpol.2010.09.025.

[17] J.F.V. Vincent, U.G.K. Wegst, Design and mechanical properties of insect cuticle, Arthropod Struct. Dev. 33 (2004) 187–199. https://doi.org/10.1016/j.asd.2004.05.006.

[18] D. Montroni, M. Palanca, K. Morellato, S. Fermani, L. Cristofolini, G. Falini, Hierarchical chitinous matrices byssus-inspired with mechanical properties tunable by Fe (III) and oxidation, Carbohydr. Polym. 251 (2021) 116984. https://doi.org/10.1016/j.carbpol.2020.116984.

[19] D. Montroni, F. Sparla, S. Fermani, G. Falini, Influence of proteins on mechanical properties of a natural chitin-protein composite, Acta Biomater. (2020). https://doi.org/10.1016/j.actbio.2020.04.039.

[20] D. Montroni, X. Zhang, J. Leonard, M. Kaya, C. Amemiya, G. Falini, M. Rolandi, Structural characterization of the buccal mass of Ariolimax californicus (Gastropoda; Stylommatophora), PLoS One. 14 (2019) e0212249.

[21] H. Ehrlich, M. Krautter, T. Hanke, P. Simon, C. Knieb, S. Heinemann, H. Worch, First Evidence of the Presence of Chitin in Skeletons of Marine Sponges. Part II. Glass Sponges (Hexactinellida: Porifera), J. Exp. Zool. (Mol Dev Evol). 308B (2007) 473–483. https://doi.org/10.1002/jez.b.

[22] P.Y. Chen, A.Y.M. Lin, J. McKittrick, M.A. Meyers, Structure and mechanical properties of crab exoskeletons, Acta Biomater. 4 (2008) 587–596. https://doi.org/10.1016/j.actbio.2007.12.010.

[23] S. Weiner, Y. Talmon, W. Traub, Electron diffraction of mollusc shell organic matrices and their relationship to the mineral phase, Int. J. Biol. Macromol. 5 (1983) 325–328. https://doi.org/10.1016/0141-8130(83)90055-7.

[24] E.C. Keene, J.S. Evans, L.A. Estroff, Matrix Interactions in Biomineralization: Aragonite Nucleation by an Intrinsically Disordered Nacre Polypeptide, n16N, Associated with a β-Chitin Substrate, Cryst. Growth Des. 10 (2010) 1383–1389. https://doi.org/10.1021/cg901389v.

[25] A.C.A. Wan, B.C.U. Tai, Chitin - A promising biomaterial for tissue engineering and stem cell

technologies, Biotechnol. Adv. 31 (2013) 1776–1785. https://doi.org/10.1016/j.biotechadv.2013.09.007.

[26] M. Abe, M. Takahashi, S. Tokura, H. Tamura, A. Nagano, Cartilage – Scaffold Composites Produced by Bioresorbable b -Chitin Sponge with Cultured Rabbit Chondrocytes, Tissue Eng. 10 (2004) 585–594.

[27] Z. Ge, S. Baguenard, L. Yong, A. Wee, E. Khor, Hydroxyapatite – chitin materials as potential tissue engineered bone substitutes, Biomaterials. 25 (2004) 1049–1058. https://doi.org/10.1016/S0142-9612(03)00612-4.

[28] G. Magnabosco, A. Ianiro, D. Stefani, A. Soldà, S. Rapino, G. Falini, M. Calvaresi, Doxorubicin-Loaded Squid Pen Plaster: A Natural Drug Delivery System for Cancer Cells, ACS Appl. Bio Mater. 3 (2020) 1514–1519. https://doi.org/10.1021/acsabm.9b01137.

[29] R. Jayakumar, A. Nair, N.S. Rejinold, S. Maya, S. V. Nair, Doxorubicin-loaded pH-responsive chitin nanogels for drug delivery to cancer cells, Carbohydr. Polym. 87 (2012) 2352–2356. https://doi.org/10.1016/j.carbpol.2011.10.040.

[30] Y. Okamoto, M. Watanabea, K. Miyatakea, M. Morimoto, Y. Shigemasa, S. Minami, Effects of Chitin/Chitosan and Their Oligomers/Monomers on Migrations of fibroblasts and vascular endothelium, Biomaterials. 23 (2002) 1975–1979. https://doi.org/10.1002/mabi.200350026.

[31] T. Mori, M. Okumura, M. Matsuura, K. Ueno, S. Tokura, Y. Okamoto, S. Minami, T. Fujinaga, Effects of chitin and its derivatives on the proliferation and cytokine production of fibroblasts in vitro, Biomaterials. 18 (1997) 947–951. https://doi.org/10.1016/S0142-9612(97)00017-3.

[32] X. Li, Q. Feng, X. Liu, W. Dong, F. Cui, Collagen-based implants reinforced by chitin fibres in a goat shank bone defect model, Biomaterials. 27 (2006) 1917–1923. https://doi.org/10.1016/j.biomaterials.2005.11.013.

[33] S.B. Lee, Y.H. Kim, M.S. Chong, Y.M. Lee, Preparation and characteristics of hybrid scaffolds

composed of β-chitin and collagen, Biomaterials. 25 (2004) 2309–2317. https://doi.org/10.1016/j.biomaterials.2003.09.016.

[34] J. Jin, P. Hassanzadeh, G. Perotto, W. Sun, M.A. Brenckle, D. Kaplan, F.G. Omenetto, M. Rolandi, A biomimetic composite from solution self-assembly of chitin nanofibers in a silk fibroin matrix, Adv. Mater. 25 (2013) 4482–4487. https://doi.org/10.1002/adma.201301429.

[35] R. Arun Kumar, A. Sivashanmugam, S. Deepthi, S. Iseki, K.P. Chennazhi, S. V. Nair, R. Jayakumar, Injectable chitin-poly(ε-caprolactone)/nanohydroxyapatite composite microgels prepared by simple regeneration technique for bone tissue engineering, ACS Appl. Mater. Interfaces. 7 (2015) 9399–9409. https://doi.org/10.1021/acsami.5b02685.

[36] M. Peter, P.T. Sudheesh Kumar, N.S. Binulal, S. V. Nair, H. Tamura, R. Jayakumar, Development of novel α-chitin/nanobioactive glass ceramic composite scaffolds for tissue engineering applications, Carbohydr. Polym. 78 (2009) 926–931. https://doi.org/10.1016/j.carbpol.2009.07.016.

[37] X. Li, Q. Feng, W. Wang, F. Cui, Chemical characteristics and cytocompatibility of collagen-based scaffold reinforced by chitin fibers for bone tissue engineering, J. Biomed. Mater. Res. - Part B Appl. Biomater. 77 (2006) 219–226. https://doi.org/10.1002/jbm.b.30425.

[38] F.Z. Cui, Y. Li, J. Ge, Self-assembly of mineralized collagen composites, Mater. Sci. Eng. R Reports. 57 (2007) 1–27. https://doi.org/10.1016/j.mser.2007.04.001.

[39] J.-H. Bradt, M. Mertig, A. Teresiak, W. Pompe, Biomimetic Mineralization of Collagen by Combined Fibril Assembly and Calcium Phosphate Formation, Chem. Mater. 11 (1999) 2694–2701. https://doi.org/10.1021/cm991002p.

[40] D. Montroni, B. Marzec, F. Valle, F. Nudelman, G. Falini, β-Chitin Nanofibril Self-Assembly in Aqueous Environments, Biomacromolecules. 20 (2019) 2421–2429. https://doi.org/10.1021/acs.biomac.9b00481.

[41] F. Valle, M. Brucale, S. Chiodini, E. Bystrenova, C. Albonetti, Nanoscale morphological analysis of soft matter aggregates with fractal dimension ranging from 1 to 3, Micron. 100 (2017) 60–72. https://doi.org/10.1016/j.micron.2017.04.013.

[42] Z. Tian, Y. Wang, H. Wang, K. Zhang, Regeneration of native collagen from hazardous waste: chrome-tanned leather shavings by acid method, Environ. Sci. Pollut. Res. 27 (2020) 31300–31310. https://doi.org/10.1007/s11356-020-09183-4.

[43] W. Liao, X. Guanghua, Y. Li, X.R. Shen, C. Li, Comparison of characteristics and fibril-forming ability of skin collagen from barramundi (Lates calcarifer) and tilapia (Oreochromis niloticus), Int. J. Biol. Macromol. 107 (2018) 549–559. https://doi.org/10.1016/j.ijbiomac.2017.09.022.

[44] K. Wu, W. Liu, G. Li, The aggregation behavior of native collagen in dilute solution studied by intrinsic fluorescence and external probing, Spectrochim. Acta - Part A Mol. Biomol. Spectrosc. 102 (2013) 186–193. https://doi.org/10.1016/j.saa.2012.10.048.

[45] K. Van De Velde, P. Kiekens, Structure analysis and degree of substitution of chitin, chitosan and dibutyrylchitin by FT-IR spectroscopy and solid state13C NMR, Carbohydr. Polym. 58 (2004) 409–416. https://doi.org/10.1016/j.carbpol.2004.08.004.

[46] K.H. Gardner, J. Blackwell, Refinement of the Structure of β-Chiti, Biopolymers. 14 (1975) 1581–1595.

[47] H. Moon, S. Choy, Y. Park, Y.M. Jung, J.M. Koo, D.S. Hwang, Different molecular interaction between collagen and α- or β-chitin in mechanically improved electrospun composite, Mar. Drugs. 17 (2019) 318. https://doi.org/10.3390/md17060318.

[48] M. Steegmaler, A. Levinovitz, S. Isenmann, E. Borges, M. Lenter, H.P. Kocher, B. Kleuser, D. Vestweber, The E-selectin-ligand ESL-1 is a variant of a receptor for fibroblast growth factor, Nature. 373 (1995) 615–620. https://doi.org/10.1038/373615a0.

[49] C.F. Brewer, M.C. Miceli, L.G. Baum, Clusters, bundles, arrays and lattices: Novel mechanisms

for lectin-saccharide-mediated cellular interactions, Curr. Opin. Struct. Biol. 12 (2002) 616–623. https://doi.org/10.1016/S0959-440X(02)00364-0.